Stress and dislocations in thin metal layers

Nicola, Lucia

Chapter 1

Discrete dislocation plasticity

Plastic deformation of crystalline metals is caused by glide of a large number of dislocations. In the case of massive pieces of material, keeping track of the motion of all the individual dislocations would be a very impractical way of measuring plastic relaxation. Fortunately, plasticity in sufficiently large samples often can be efficiently described by continuum models, which neglect the discrete nature of dislocations and only account for the effect of their collective motion. This is made possible by the fact that dislocations are so small with respect to the dimensions of the sample.

However, when one of the dimensions of the specimen is at the micrometer scale, these requirements stop being valid and continuum models may cease to be useful. In confined small structures, dislocation loops cannot form and move as freely as in bulk metal. Moreover, the patterns that dislocations form in order to reduce the stress state in the material, can be comparable in size to the size of the sample itself. If this happens, the stress state associated to the patterning needs to be taken into account.

The above forms the motivation to study plasticity in thin metal films using a model that considers all the dislocations which are generated during the deformation process, their stress and strain fields, their motion and their interactions.

1.1 About the method

Various discrete dislocation models have been presented in the last 15 years which describe individual dislocations as line singularities in an elastic medium, e.g. [1]–[10]. This seems to be a good representation of a dislocation beyond 10 atomic distances from the dislocation core [11, 12, 13]. The framework we will use in this thesis is the one formulated in 1995 by Van der Giessen and Needleman [14] to solve quasi-static boundary value problems for dislocated bodies. It is based on the formulation of Lubarda et al. [5] for equilibrium dislocation arrangements:

stress, strain and displacement fields in the body are given as superposition of the fields describing the dislocations as if they were singularities in an infinite elastic body and complementary fields which enforce the prescribed boundary conditions on the actual body. The Van der Giessen-Needleman approach describes the evolution of the dislocation structure during quasi-static deformation of the body. This is done by using constitutive rules for dislocation glide, nucleation and annihilation of the kind proposed by Kubin [3]. The simulations follow an incremental procedure: at each time step the fields are calculated in the body and then the dislocation structure is updated.

1.1.1 The dislocated body at a given time increment

At a generic time of deformation the body contains a certain distribution of dislocations, see Fig. 1.1(a). They are regarded as line defects in the body which is elsewhere described as a linear elastic continuum. At the boundary $S = S_u \cup S_f$ mixed periodic boundary conditions are prescribed: S_f is the portion of the boundary on which tractions $\boldsymbol{T}_0$ are prescribed, S_u is the portion of the boundary on which displacements $\boldsymbol{u}_0$ are prescribed and $\boldsymbol{n}$ is the outer unit normal to S.

As shown in Fig. 1.1 the current state of the body in terms of the displacement, strain and stress fields is calculated as the sum of two contributions:

$$\boldsymbol{u} = \tilde{\boldsymbol{u}} + \hat{\boldsymbol{u}}\,, \quad \boldsymbol{\varepsilon} = \tilde{\boldsymbol{\varepsilon}} + \hat{\boldsymbol{\varepsilon}}\,, \quad \boldsymbol{\sigma} = \tilde{\boldsymbol{\sigma}} + \hat{\boldsymbol{\sigma}}\,. \tag{1.1}$$

Here, the $(\tilde{\ })$-fields are the superpositions of the fields of the individual dislocations as if they were in in infinite space,

$$\tilde{\boldsymbol{u}} = \sum_I \boldsymbol{u}^{(I)}\,, \quad \tilde{\boldsymbol{\varepsilon}} = \sum_I \boldsymbol{\varepsilon}^{(I)}\,, \quad \tilde{\boldsymbol{\sigma}} = \sum_I \boldsymbol{\sigma}^{(I)}\,. \tag{1.2}$$

(the superscript (I) denotes the Ith dislocation), and are singular at the positions of the dislocations. The analytical expression for these infinite-body fields can be found in textbooks [15, 16].

The $(\hat{\ })$-fields in (1.1) represent the image fields that correct for the actual boundary conditions on S. Provided that the displacement fields are continuous on S_u, the $(\hat{\ })$-fields are smooth and can therefore be solved for by numerical techniques such as the finite element method. The governing equations for the $(\hat{\ })$ fields are

$$\left.\begin{array}{l} \nabla \cdot \hat{\boldsymbol{\sigma}} = \boldsymbol{0} \\ \hat{\boldsymbol{\varepsilon}} = \mathrm{sym}(\nabla \otimes \hat{\boldsymbol{u}}) \end{array}\right\} \text{ in } V \tag{1.3}$$

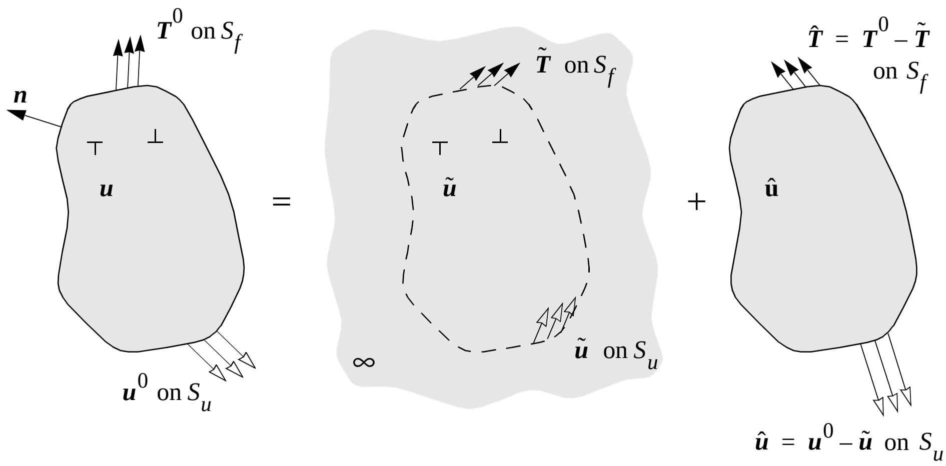

Figure 1.1 Decomposition of the problem for the dislocated body into the problem of interacting dislocations in the homogeneous infinite solid ((˜)-fields) and the complementary problem for the nonhomogeneous body without dislocations ((ˆ)-fields).

$$\hat{\boldsymbol{\sigma}} = \boldsymbol{\mathcal{L}} : \hat{\boldsymbol{\varepsilon}} \quad \text{in } V \tag{1.4}$$

$$\begin{aligned} \boldsymbol{n} \cdot \hat{\boldsymbol{\sigma}} = \hat{\boldsymbol{T}} = \boldsymbol{T}_0 - \tilde{\boldsymbol{T}} \quad & \text{on } S_f \\ \boldsymbol{u} = \hat{\boldsymbol{U}} = \boldsymbol{u}_0 - \tilde{\boldsymbol{U}} \quad & \text{on } S_u \end{aligned} \tag{1.5}$$

Here, $\boldsymbol{\mathcal{L}}$ is the tensor of elastic moduli of the body, which is taken to be isotropic. While the formulation holds in general, the problems addressed in this thesis are two dimensional.

1.2 The evolving dislocation ensemble

The connection between the stress state in the body and the evolution of the dislocation structure is made by a set of constitutive rules. These rules relate the resolved shear stress on the slip planes in the body to the dislocation activity. The constitutive relations control nucleation, glide, annihilation and pinning of dislocations at an obstacle. Figure 1.2 shows schematically the main steps of the program used to simulate dislocation dynamics.

1.2.1 Nucleation

Nucleation occurs by activation of Frank-Read sources, already present in the material due to previous plastic activity. The dislocation sources are positioned on the slip planes and their density is taken to be constant during the simulation. A certain stress must act on a source to make it operate by bowing out the Frank-Read segment and form a new dislocation loop.

In the two-dimensional formulation used in this thesis, we just consider traces of the slip planes intersecting the plane of deformation and Frank-Read segments are approximated as point sources on those traces. The dislocation loop generated by the source, intersects the plane of deformation in two points. Assuming that the loop opens and expands symmetrically with respect to the source, these two points are two purely edge dislocations of opposite sign. Since relaxation of thin films is controlled by glide of the straight part of dislocation loops, keeping track of the motion of edge dislocations pairs seems to be an appropriate way to approach the thin film problem in two dimensions.

Three parameters are associated to each source: a critical strength τ_{nuc} necessary to create the new dislocation loop, the critical time t_{nuc} required for its formation and the diameter of the loop at nucleation, L_{nuc}. This distance is such that the attractive stress field that the dislocations exert on each other is equilibrated by the resolved shear stress at nucleation (τ_{nuc}),

$$L_{\mathrm{nuc}} = \frac{\mu}{2\pi(1-\nu)} \frac{b}{\tau_{\mathrm{nuc}}} . \tag{1.6}$$

1.2.2 Glide

Glide of the dislocation loop on the slip plane is driven by the Peach-Koehler force. The component of the Peach-Koehler force acting on the I-th dislocation is

$$f^{(I)} = \boldsymbol{n}^{(I)} \cdot (\hat{\boldsymbol{\sigma}} + \sum_{J \neq I} \boldsymbol{\sigma}^{(J)}) \cdot \boldsymbol{b}^{(I)} , \tag{1.7}$$

where $\boldsymbol{t}^{(I)}$ is the unit vector tangent to the I-th dislocation line and $\boldsymbol{b}^{(I)}$ is its Burgers vector. For edge dislocations equation 1.7 reduces to:

$$f^{(I)} = \tau^{(I)} b^{(I)}, \tag{1.8}$$

where τ^{I} is the resolved shear stress on the slip plane containing dislocation I.

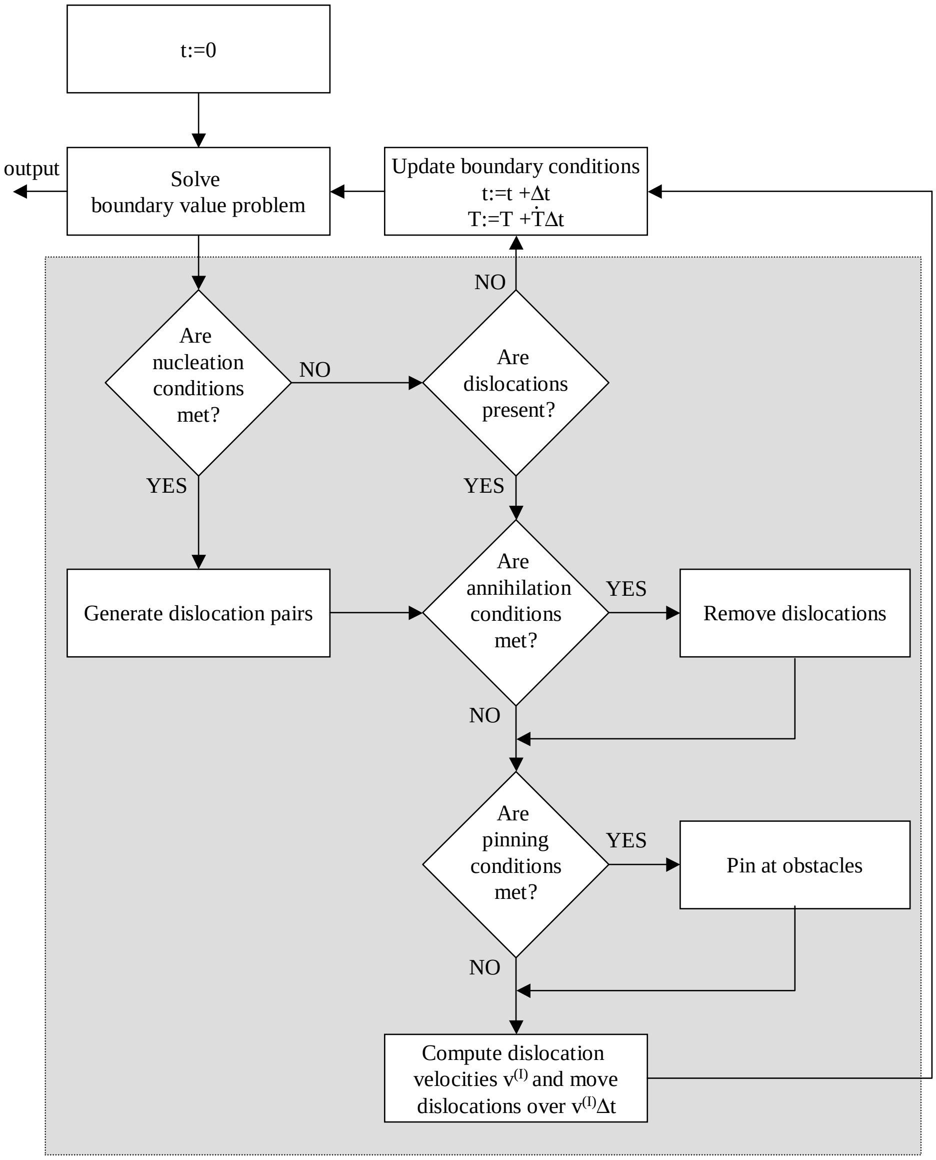

Figure 1.2 Schematic representation of the program. The computations which treat dislocation dynamics are listed in the gray box.

In this quasi-static framework glide is assumed to be drag controlled; thus the velocity of dislocation I, v^I, in the direction of $\boldsymbol{s}^I$ is proportional to the resolved shear stress according to the drag relation

$$\tau^{(I)}b^{(I)} = Bv^{(I)} \tag{1.9}$$

with B the drag coefficient.

1.2.3 Pinning at obstacles

Dislocation glide can be hindered in real metals by different kinds of obstacles like precipitates, grain boundaries or other dislocations on intersecting slip planes. In principle it is possible to map the defects with their properties from a three dimensional crystal into a two dimensional representation [17]. Here, the obstacles are just modeled as point obstacles on the slip planes at which dislocations get pinned. Each obstacle is characterized by a critical strength, τ_{obs}. As long as the resolved shear stress acting on the pinned dislocation is lower than the obstacle strength, the dislocation cannot overtake the obstacle. Often the presence of an obstacle causes the formation of a dislocation pile-up which induces a high shear stress on the leading dislocation. If the shear stress exceeds the critical strength of the obstacle, the dislocation is released.

1.2.4 Annihilation

Occasionally, dislocation loops collapse on themselves, because the stress state which caused their nucleation suddenly decreases, or is not sufficiently large to promote their growth. When this happens the couple of opposite signed edge dislocations (which represent the loop's cross-section) approach each other until they annihilate. This is modeled by removing dislocations of opposite sign from the simulation when they are on the same slip plane closer to each other than the critical material-dependent distance L_{ann}.

References

[1] A.N. Gulluoglu, D.J. Srolovitz, R. LeSar and P.S. Lomdahl, Scripta Metall. **23** (1989) 1347.

[2] R.J. Amodeo and N.M. Ghoniem, Phys. Rev. B **41** (1990) 6968.

[3] L.P. Kubin, G. Canova, M. Condat, B. Devincre, V. Pontikis and Y. Bréchet, in Nonlinear Phenomena in Materials Science II (edited by G. Martin and L.P. Kubin), Sci-Tech, Vaduz (1992) 455.

[4] A.N. Gulluoglu and C.S. Hartley, Model. Simul. Mater. Sci. Eng. **1** (1993) 383.

[5] V. Lubarda, J.A. Blume and A. Needleman, Acta Metall. Mater. **41** (1993) 625.

[6] X.F. Fang and W. Dahl, Mater. Sci. Eng. **A164** (1993) 300.

[7] I. Groma and G.S. Pawley, Mater. Sci. Eng. **A164** (1993) 306.

[8] Y. Bréchet, G. Canova, L.P. Kubin, Acta Mater. **44** (1996) 4261.

[9] M.C. Fivel, T.J. Gosling, G.R. Canova, Model. Simul. Mater. Sci. Eng. **4** (1996) 581.

[10] H.M. Zbib, M. Rhee and J.P. Hirth, Int. J. Mech. Sci. **40** (1998) 113.

[11] H.C. Choi, A.F. Schwartzman and K.-S. Kim, Mater. Sci. Symp. Proc. **239** (1992) 419.

[12] V. Vitek, Prog. Mat. Sci. **3** (1992) 1.

[13] R. Gallego, M. Ortiz, Model. Simul. Mater. Sci. Eng. **1** (1993) 383.

[14] E. Van der Giessen, A. Needleman, Simul. Mater. Sci. Eng. **3** (1995) 689.

[15] F.R.N. Nabarro, Theory of crystal dislocations, (Oxford: Oxford University Press) (1967).

[16] J.P. Hirth and J. Lothe, Theory of dislocations, (New York: McGraw-Hill) (1968).

[17] A. Roos, J.Th.M. De Hosson, E. Van der Giessen, Computational Material Science **20** (2001) 19.